

Figure 2: Photograph of copper window and iris with distribution of RF breakdown damage spots, marked with crosshairs using ImageJ software.

All Season Cavity

Another cavity tested at the MTA known as the All Seasons cavity, is shown in Fig.3 [6]. This cavity was designed for both vacuum (3×10^{-8} Torr) and 100 atm compressed hydrogen gas operation. It consists of a SS316 cylindrical body [Fig. 3(b)] of outer diameter 366.9 mm and two end plates. The top [Fig.3(c)] and bottom [Fig. 3(d)] both have a diameter of 290.7 mm.

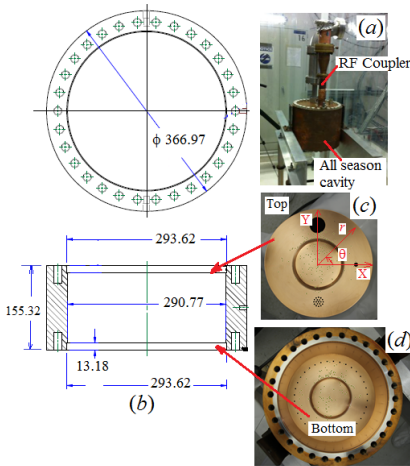


Figure 3: (a) All Seasons cavity (b) cross sectional view (c) top plate (d) bottom plate with cylindrical wall.

RF power was fed to the cavity through a coax coupler [Fig. 3(a)] with 20 μ s pulse duration and 15 Hz repetition rate. The cavity was operated at peak electric field of 25 MV/m with RF power 1.2 MW, B=0 T and 22 MV/m with RF power 0.93 MW, B= 3T magnetic field [7].

ANALYSIS AND RESULTS

LBNL-Pillbox Cavity

For the sake of analysis, the surface of the pillbox cavity window was divided into 3 regions as shown in Fig. 1(b). Region I is a circular area of radius 66.7 mm, region II is a ring of inner radius 66.7 mm and outer radius 80 mm. Both region I and region II are part of flat circular window. Region III (iris) is also a ring of inner radius 80 mm and outer radius 97.9 mm. The center of the window is the origin of the coordinate system (X, Y or

r, θ) shown in Fig.2 where Breakdown Damage (BD) spot locations are identified by crosshairs using the image processing software ImageJ. The BD spot distribution is calculated with the help of Mathematica software. Figure 4(a) shows the BD spot distribution in the X-Y plane. The upper half of the iris is close to the RF coupler and has more damage spots than the lower half. The BD spot distribution in $r-\theta$ plane is shown in Fig. 4(b).

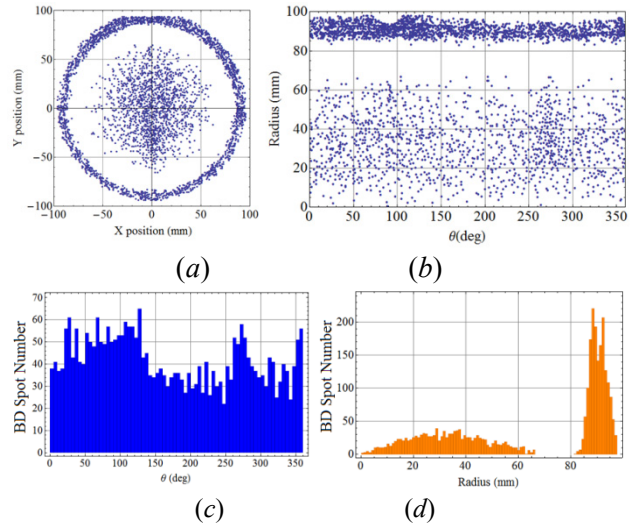


Figure 4: BD spot distribution in X-Y plane (a) and $r-\theta$ plane (b), BD spot no. vs θ plot (c) with bin size: 5 $^\circ$ and BD spot no. vs r plot (d) with bin size 0.9 mm.

The number of BD spots at different values of θ and r are depicted in Fig. 4(c) and Fig. 4(d) respectively. The electric field distribution was calculated using computer code [8] and field emission dark current density was calculated from the Fowler-Nordheim equation where we have taken the work function (ϕ) for copper to be 4.65 eV and the field enhancement factor (β) to be 200. Figure 5 illustrates the results of the electric field, dark current density and number of BD spot density. Figure 6 shows the BD spot density vs electric field in the window area. The solid circles represent the data obtained from image processing and the line indicates an electric field (E^n) power fit. This shows the data fit well with $E^{6.28}$.

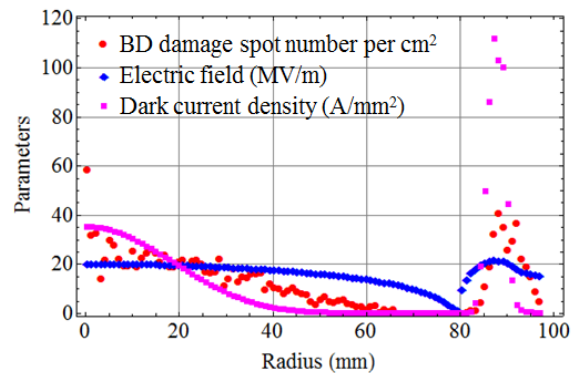


Figure 5: BD spot number per cm^2 , RF electric field and dark current density vs radial distance plot.

Copyright © 2013 CC-BY-3.0 and by the respective authors

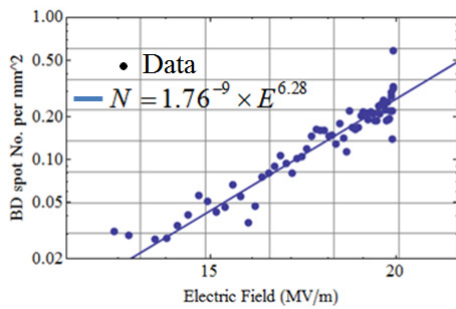


Figure 6: BD spot density vs electric field plot for flat window area.

All Seasons Cavity

Distributions of BD spot are shown in X-Y [Fig. 7(a)] and r-θ plane [Fig. 7(b)]. The number of BD spots at different values of θ and r are shown in Figs. 7(c) and 7(d) respectively. Fig. 8(a) illustrates the BD spot no. per mm² at different radii for the top plate at given θ values and Fig. 8(b) shows the same for the bottom plate. Fig. 9 depicts the computed electric field (with 10 times magnification) distribution and dark current density distribution. This is the same for both plates.

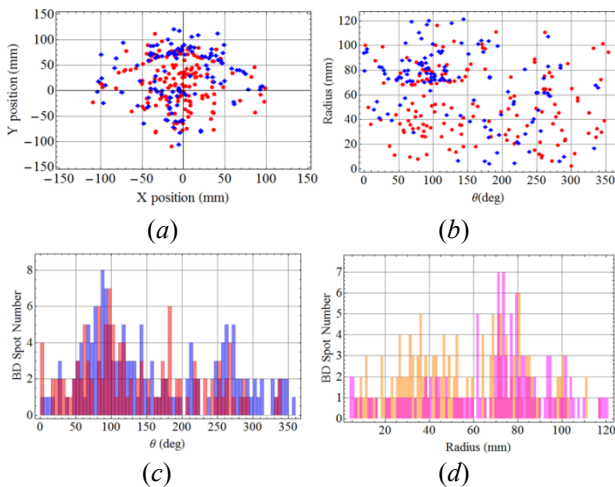


Figure 7: BD spot distribution in X-Y plane (a) and r-θ plane (b) (in both plots red/blue for top/bottom plate), BD spot no. vs θ plot (c) [blue/brown for top/bottom plate with bin size 5°], BD spot number vs r plot (d) [orange/magenta for top/bottom plate with bin size 1.2 mm].

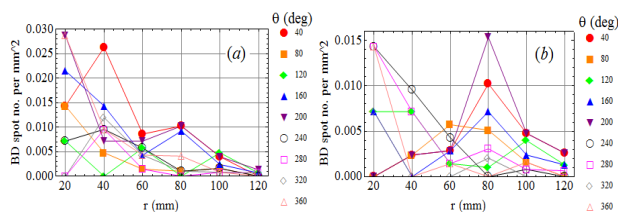


Figure 8: Plot of BD spot number per mm² at different radius for given θ (e.g. Red Circle for 40°, Orange Square for 80° and so on) (a) for top plate and (b) for bottom plate.

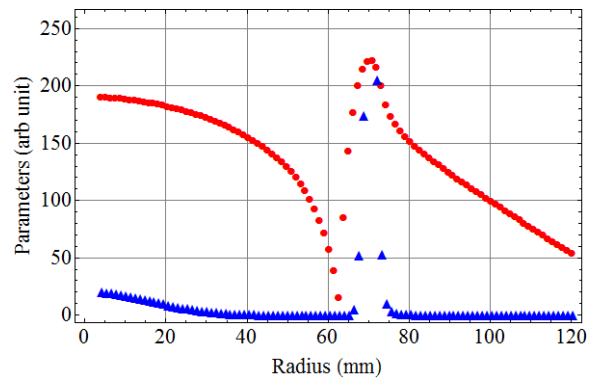


Figure 9: Electric field and dark current density distribution at different radii.

CONCLUSIONS

The BD spot distributions in both cavities are generally consistent with the electric field profiles but there are some differences. In the LBNL-Pillbox cavity, BD spots were distributed more densely over the iris region where the electric field and dark current are high. Note that the iris region includes accumulated damage from more runs than the window. In the flat window region the BD spot density data correlates with 6.28th power of the electric field. In the All Season cavity, fewer damage spots are observed because the surface inspection was carried out at an early stage of the run. In both plates most of the spots are within a radius of 100 mm. Note that in both cavities, data was taken both with and without magnetic field before the surface inspection. In future experiments, inspection will be done separately after runs with and without magnetic field to explore the role of magnetic field in the breakdown process.

REFERENCES

- [1] J. Norem et al., Phys. Rev. ST Accel. Beams 6 (2003) 072001.
- [2] A. Moretti et al., Phys. Rev. ST Accel. Beams 8 (2005) 072001.
- [3] D. Li et al., “Design and fabrication of an 805 MHz Rf cavity with Be windows for a high RF power testing for Muon cooling experiment”, Proceedings of PAC 2001, Chicago, USA, p. 918 (2001).
- [4] W.S. Rasband, “ImageJ”, U.S. National Institute of Health, Bethesda, Maryland, USA, <http://rsb.info.nih.gov/ij> (1997-2010).
- [5] Wolfram Research, Inc. USA, www.wolfram.com
- [6] G. Kazakevich et al., “Conditioning and future plans for a multi-purpose 805 MHz pillbox cavity for Muon acceleration”, Proceedings of IPAC 2012, New Orleans, USA, THPPC032, p. 3353 (2012).
- [7] Y. Torun et al., “Extended RF Testing of the 805 MHz Pillbox “All-Season” cavity for Muon Cooling”, WEPMA17, NA-PAC’13.
- [8] A. Moretti, Fermilab, USA (private communication).